

## N O T I C E

THIS DOCUMENT HAS BEEN REPRODUCED FROM  
MICROFICHE. ALTHOUGH IT IS RECOGNIZED THAT  
CERTAIN PORTIONS ARE ILLEGIBLE, IT IS BEING RELEASED  
IN THE INTEREST OF MAKING AVAILABLE AS MUCH  
INFORMATION AS POSSIBLE

*JF*  
NASA Technical Memorandum 81751

(NASA-TM-81751) HIGH-FREQUENCY SOUND  
PROPAGATION IN A SPATIALLY VARYING MEAN FLOW  
(NASA) 29 p HC A03/MF A01 CSCL 20A

N81-20831

Unclassified  
G3/71 41915

# High-Frequency Sound Propagation in a Spatially Varying Mean Flow

Y. C. Cho and E. J. Rice  
*Lewis Research Center*  
*Cleveland, Ohio*



Prepared for the  
One-hundredth Meeting of the Acoustical Society of America  
Los Angeles, California, November 17-21, 1980

NASA

**High-frequency sound propagation in a spatially varying mean flow**

**Y. C. Cho and E. J. Rice  
NASA Lewis Research Center  
Cleveland, Ohio 44135**

**Received \_\_\_\_\_**

## ABSTRACT

An equation for acoustics ray paths in a spatially varying mean flow has been examined to determine some of the characteristics of the flow gradient effects on sound propagation. In a potential flow the acoustic rays are deflected in the direction of increasing mean flow, and the gradient of the mean flow speed is the dominant factor causing the ray deflection. In contrast, in a sheared mean flow, the vorticity is the dominant factor in deflection of the acoustic rays.

## SYMBOLS

$b$	impact parameter, perpendicular distance between vortex center and incident ray
$b_m$	minimum impact parameter, smallest value of $b$ for which ray propagates without hitting cylinder wall
$c$	local sound speed
$c_\infty$	stagnation sound speed
$k$	wave number, $ k $
$\vec{k}$	wave number vector
$\hat{n}$	unit vector normal to wave front
$r$	radial distance
$r_c$	smallest radial distance from center to ray path or particle trajectory
$r_0$	radius of circular cylinder
$t$	time (variable)
$u$	mean flow speed, $ \vec{u} $
$\vec{u}$	mean flow velocity
$u_{\max}$	greatest mean flow speed on ray path
$u_0$	mean flow speed at $r = r_0$

$\vec{v}$	ray group velocity
$\hat{\vec{x}}$	unit vector parallel to x-axis
$\vec{x}$	position vector
( $x, y$ )	Cartesian coordinates (Incident rays are all chosen to be parallel to x-axis.)
$\gamma$	specific heat ratio (1.4 for air)
$\theta$	polar angle or ray deflection angle
$\theta_c$	value of $\theta$ at turning point of ray path or particle trajectory
$\hat{\theta}$	counterclockwise unit vector
$\sigma$	deflection cross section (Eq. (14))
$\omega$	angular frequency of sound (constant)
$\omega_r$	relative angular frequency (dependent on mean flow and wave number vector)

#### INTRODUCTION

This paper presents an initial theoretical investigation involving the refraction of sound within an inlet duct, such as in an aircraft jet engine system. Such an inlet duct often involves nonuniform mean flow: The flow into an inlet is nonuniform radially as well as axially;<sup>1</sup> flow in the vicinity of the inlet lip can be crudely simulated as a free vortex at least in static test conditions. One major effect of a flow gradient is the deflection of sound. In an effort to understand some of the characteristics of such an effect, the present paper examines acoustic ray paths in a simple potential flow - a free vortex with a hard-wall cylinder core. The analysis uses a geometric theory based on the eikonal equation.<sup>2</sup>

Although it is a high-frequency approximation, the geometric theory have some advantages: Since its formulation is similar to classical mechanics dealing with the motion of a particle, one can gain a direct physical

insight into the problem. It is simple and well suited to numerical computation. Furthermore the geometric theory may be able to correctly determine locations of the maximums of a duct-mode radiation pattern even for a finite frequency. The theory may possibly be expanded for more detailed radiation patterns by using a statistical interpretation of sound<sup>3</sup> or possibly by carrying out higher order calculations.<sup>4</sup>

Similar ray calculations were previously reported. Salant's calculation includes a free vortex.<sup>5</sup> He has implicitly neglected the mean flow dependence of the sound speed by assuming that the index of refraction is unity. The assumption is not consistent with the fact that in potential flow the sound speed depends on the local mean flow speed. The present calculation shows that the mean flow dependence of the sound speed exerts a significant influence on acoustic ray deflection. Georges used a somewhat different vortex model that includes shear.<sup>6</sup> The inclusion of shear results in a refraction pattern that differs considerably from the present calculation.

#### ANALYSIS

An equation is derived herein that governs the acoustic ray paths in a spatially varying mean flow. The mean flow is assumed to be isentropic. The derivation can be considered as a review, and thus no justifications will be detailed. Instead, refer to the following references: The fundamentals of the geometric theory of waves are given in books by Landau and Lifshitz<sup>2</sup> and by Born and Wolf;<sup>7</sup> ray tracing in a moving medium is discussed in a book by Lighthill<sup>8</sup> and papers by Blokhintzev,<sup>9</sup> Brettherton and Garret,<sup>10</sup> Candel,<sup>11</sup> and Hayes.<sup>12</sup>

Let us begin with the well-known dispersion relation of sound in flow<sup>13</sup>

$$\omega = ck + \hat{u} \cdot \hat{k} \quad (1)$$

where  $\omega$  is the angular frequency of the sound,  $c$  the local sound speed,  $\vec{u}$  the mean flow velocity,  $\vec{k}$  the wave number vector, and  $k = |\vec{k}|$ . In Ref. 3,  $\omega_r$ , called the relative frequency therein, is used in place of  $ck$ .

The time derivative of the two conjugate variables,  $\vec{k}$  and the position vector  $\vec{x}$ , is obtained by means of the Hamilton-Jacobi equation as follows:

$$\dot{\vec{x}} = \frac{\partial \omega}{\partial \vec{k}}, \quad \dot{\vec{k}} = -\vec{v}\omega. \quad (2a, b)$$

Here the dot over  $\vec{x}$  and  $\vec{k}$  stands for the total time derivative. In general, the total time derivative of a function  $\vec{f}(\vec{x}, \vec{k}, t)$  is obtained as

$$\dot{\vec{f}} \equiv \frac{d\vec{f}}{dt} = (\dot{\vec{x}} \cdot \vec{\nabla})\vec{f} + \left( \dot{\vec{k}} \cdot \frac{\partial}{\partial \vec{k}} \right) \vec{f} + \frac{\partial \vec{f}}{\partial t}.$$

It follows from Eqs. (1) and (2a) that

$$\dot{\vec{x}} = \vec{v} = c\hat{n} + \vec{u} \quad (3)$$

where  $\hat{n} = \vec{k}/k$  is the unit vector normal to the wave front. From Eqs. (1) and (2b)

$$\dot{\vec{k}} = -k\vec{v}c - (\vec{k} \cdot \vec{v})\vec{u} - \vec{k} \times \vec{v} \times \vec{u}. \quad (4)$$

The local speed of sound in isentropic flow is given by<sup>13</sup>

$$c^2 = c_\infty^2 - \frac{\gamma - 1}{2} u^2, \quad (5)$$

where  $c_\infty$  is the stagnation sound speed and  $\gamma$  the specific heat ratio of the fluid.

A numerical integration method can be immediately applied to Eqs. (3) to (5) to determine acoustic ray paths for a given mean flow and initial conditions. Before going into details of the numerical solutions, we will qualitatively discuss the kinematics of the acoustic ray. To this end, we combine Eqs. (3) and (4). Taking the total time derivative of Eq. (3) yields

$$\dot{\vec{v}} = \vec{c}\hat{n} + c\dot{\hat{n}} + \dot{\vec{u}}. \quad (6)$$

Inserting Eqs. (3) to (5) into Eq. (6) gives

$$\dot{\vec{v}} = \frac{1+1}{4} \vec{v} u^2 - \vec{v} \times \vec{v} \times \vec{u} + \hat{n} g, \quad (7)$$

where  $g$  is a scalar function given by

$$g = (2\vec{v} - \vec{u}) \cdot \vec{\nabla} c + \hat{n} \cdot (c\hat{n} \cdot \vec{\nabla})\vec{u}. \quad (8)$$

In deriving Eq. (7), we have also used

$$\dot{c} = \vec{v} \cdot \vec{\nabla} c, \quad \dot{\vec{u}} = (\vec{v} \cdot \vec{\nabla})\vec{u}, \quad \dot{\vec{k}} = \vec{k} \cdot \vec{\nabla}/k, \quad \dot{\hat{n}} = (\vec{k} - \hat{n}\vec{k})/k. \quad (9)$$

Equation (7) may be viewed as the equation of motion for a wave packet in a spatially varying mean flow. The acceleration  $\dot{\vec{v}}$  of the wave packet has been separated into three terms on the right side of Eq. (7). The acceleration represented by the first term is proportional to the gradient of the square of the mean flow speed and is independent of the wave packet motion. Note that this acceleration is in the direction of the maximum increase of the square of the mean flow speed. The acceleration in the second term is caused by the vorticity and is perpendicular to the group velocity (or the wave packet motion). All the remaining contributions are put together in the third term. This acceleration is normal to the wave front.

Consider the limiting case of  $u/c \ll 1$ , for which Eq. (7) can be written, to the first-order approximation, as

$$\dot{\vec{v}} = -\vec{v} \times \vec{\nabla} \times \vec{u} + \frac{\vec{v}}{c^2} \{ \vec{v} \cdot (\vec{v} \cdot \vec{\nabla})\vec{u} \}. \quad (10)$$

Here the last term represents the acceleration parallel to the group velocity. Thus the ray deflection is, in this case, caused only by the vortic-

ity. In other words an acoustic ray is hardly deflected in a potential flow of low Mach number.

For a potential flow of high Mach number, Eq. (7) is written as

$$\ddot{\mathbf{v}} = \frac{\gamma + 1}{4} \nabla u^2 + \frac{\hat{n}}{c} \left\{ -\frac{\gamma + 1}{2} (\dot{\mathbf{v}} \cdot \nabla) u^2 + \dot{\mathbf{v}} \cdot (\nabla \cdot \dot{\mathbf{v}}) \mathbf{u} \right\} \quad (11)$$

The numerical solutions of this equation are discussed in the next section.

#### NUMERICAL RESULTS AND DISCUSSION

In this section, numerical solutions of Eq. (11) are presented for a mean flow that is composed of a free vortex with a hard-wall circular cylinder core. The cylinder core is included here for two purposes: (1) to simulate a hard-wall boundary; and (2) to avoid the flow singularly at the vortex center.

The mean flow is described as

$$\mathbf{U} = \frac{u_0 r_0}{r} \hat{\theta} \quad \text{for } r \geq r_0, \quad (12)$$

where  $r$  is the radial distance from the cylinder axis,  $r_0$  the radius of the cylinder core,  $u_0$  the mean flow speed at  $r = r_0$ , and  $\hat{\theta}$  the counterclockwise unit vector.

For comparison, the discussion also includes trajectories of a classical particle of unit mass moving under the potential given in the form  $-(\gamma + 1)u^2/4$ . The equation of the motion of the particle is then

$$\ddot{\mathbf{v}} = \frac{\gamma + 1}{4} \nabla u^2. \quad (13)$$

The solution of this equation can be obtained in a closed form for  $\mathbf{u}$  given in Eq. (12)<sup>14</sup> and is reviewed in the Appendix.

If the second term on the right side of Eq. (11) is smaller than the first term, Eq. (13) will be an approximate equation for acoustic ray prop-

agation in a potential flow. It is not easy to determine whether the second term is negligible. However, the numerical results presented herein show that the particle trajectory is almost the same as the ray path of downstream propagation and that the upstream ray path, although differing from the particle trajectory, is also characteristically similar to it.

In Fig. 1, the pattern of the acoustic ray propagation is portrayed for the case of  $u_0/c_\infty = 0.5$ . All the rays are initially parallel to the x-axis. A ray is specified in terms of the impact parameter  $b$ , which is defined as the perpendicular distance from the vortex center ( $r = 0$ ) to the initial group velocity of the ray. Given at the end of each ray is the deflection angle  $\theta$ , which is defined as the angle difference between the initial and the final group velocities of the ray. The ray deflection is small for large values of  $b$ . As the value of  $b$  decreases, the deflection increases. There exists a minimum value of  $b$  for which the ray may propagate through without hitting the cylinder wall. As is shown later, the minimum value of  $b$ , denoted by  $b_m$ , is always greater than  $r_0$  and depends on the mean flow  $u_0/c_\infty$ . It also depends on whether the ray is initially above or below the x-axis. In determining the ray path for  $b < b_m$ , we have used the usual rule of the sound reflection from a hard wall in addition to Eq. (11).

One of the more important findings from Fig. 1 is that all the rays are deflected toward the vortex center. This phenomenon is an acoustic ray characteristic of the free vortex and can be accounted for principally by the term  $\nabla u^2$  in Eq. (11). For the free vortex this term constitutes the centerward acceleration of the wave packet. The acceleration is inversely proportional to the third power of the radial distance  $r$  from the vortex center. The acoustic ray path for  $b > b_m$  is somewhat similar to the

open trajectory of a particle moving under a similar attractive central force field (see Appendix). Note that the second term on the right side of Eq. (11) is smaller than the first, at least for  $b > b_m$ , and is negligible in the vicinity of the turning point (point of closest approach).

Also note that the deflection is greater for upstream rays than for downstream rays. This result contrasts somewhat to the ray deflection in a viscous vortex, which was considered in Ref. 6 (cf. Fig. 2 in the reference). In a viscous flow the wave packet acceleration due to vorticity is likely to be a dominant factor for the ray deflection, as can be noted from Eqs. (7) and (10). On the other hand, in the absence of vorticity, the term  $\nabla u^2$  is the dominant factor. The group velocity is smaller for the case of upstream propagation than for downstream propagation, while the centerward acceleration represented by the first term in Eq. (11) is independent of the group velocity. Consequently, a wave packet experiences longer centerward acceleration, and greater ray deflection results for upstream propagation than for downstream propagation.

Plotted in Fig. 2 is the relation between the mean flow speed  $u_0/c_\infty$  at  $r = r_0$  and the minimum impact parameter  $b_m/r_0$ . As expected,  $b_m$  is close to  $r_0$  for low mean flow speeds ( $u_0/c_\infty \ll 1$ ). As the mean flow speed increases,  $b_m$  increases slowly at first, and the relation eventually becomes almost linear. Both  $b_m$  and its slope are larger for upstream propagation than for downstream propagation. Note that the  $b_m$  vs.  $u_0$  relation for particle motion, which is computed from Eq. (A9), is almost the same as that for downstream ray propagation. The results in this figure can be used in ray theoretical studies of the sound radiation directivity from an inlet duct. It is important in such studies to determine whether a ray may propagate through the inlet flow with or without being

reflected near the inlet lip. According to the present result the probability that a ray will hit the inlet lip is enhanced with the presence of a free-vortex-like flow near the lip.

In Fig. 3 the ray deflection angle  $\theta$  is plotted as a function of the mean flow speed  $u_0/c_\infty$  for three values of the impact parameter  $b/r_0$ . As mentioned earlier (in the paragraph following Eq. (10)), the deflection is negligible near  $u_0 = 0$ . As the mean flow speed increases, the deflection angle increases. The increase is faster for the smaller impact parameter. The deflection is larger for upstream rays than for downstream rays. The result for the particle motion is again almost the same as that for the downstream ray propagation. For  $b/r_0 = 3$  and 6 the results for particle motion, which are not shown, are almost identical to those for downstream propagation.

In Fig. 4 the deflection angle  $\theta$  is plotted as a function of the impact parameter  $b/r_0$ . Each curve begins with  $b \approx b_m$ . The ray deflection is the greatest at  $b = b_m$  and decreases rapidly in the beginning with increasing impact parameter. The deflection eventually becomes negligible for large values of  $b/r_0$ . Again, the upstream rays experience greater deflection than the downstream rays. The deflection of a downstream ray is almost the same as that of a particle.

The slope of the curves in Fig. 4 can be used to determine the intensity of the deflected ray. To this end, one may define the deflection cross section  $\sigma$  as follows:  $\sigma r_0 d\theta$  is the total power of the rays deflected into the angle  $d\theta$  at  $\theta$  for unit intensity of the incident ray within  $db$  at  $y = b$ . For a fixed value of  $u_0/c_\infty$ ,  $\theta$  is a single-valued function of  $b$ , and vice versa. Thus the cross section is obtained as

$$\sigma = \frac{1}{r_0} \frac{db}{d\theta}. \quad (14)$$

where  $r_0$  is used to nondimensionalize  $\sigma$ . Note that  $\sigma$  is the inverse of the slope of the curves in Fig. 4 and is proportional to the intensity of the deflected rays. One may refer to Section 3.7 in Ref. 14 for more information on the cross section.

In Fig. 5 the deflection cross section  $\sigma$  is plotted as a function of the impact parameter  $b/r_0$ . Each curve begins with  $b = b_m$ . The cross section is almost zero at  $b = b_m$  and increases with increasing impact parameter. It increases also with decreasing mean flow speed  $u_0/c_\infty$ . Note also that the cross section is greater for downstream rays than for upstream rays. The result for the particle motion is again found to be almost the same as that for downstream ray propagation unless the impact parameter is too large.

If the intensity distribution of the incident rays is known as a function of  $b$ , the angle intensity distribution of the deflected rays can be determined from curves such as those given in Figs. 4 and 5. It is sometimes convenient to express the cross section as a function of the deflection angle, as in Fig. 6. In this figure,  $\sigma/(u_0/c_\infty)$  is used in place of  $\sigma$  (cf. Eq. (A11)). Each curve, corresponding to upstream or downstream rays, includes three mean flow speeds (i.e.,  $u_0/c_\infty = 0.5, 1, 1.5$ ). In other words, when divided by the factor  $u_0/c_\infty$ , the deflection angle dependence of  $\sigma$  is not changed by the variation of the mean flow speed. Note also that the results are almost the same for upstream rays, downstream rays, and particle motion.

As may be noted from Figs. 3-5 as well, the cross section is greater for smaller deflection angles. As an extreme example, the cross section  $\sigma$  is infinite with no deflection ( $\theta = 0$ ) as in the case of  $b = \infty$  or  $u_0 = 0$ . As the deflection angle increases, the cross section decreases

very rapidly in the beginning. The decreasing rate gradually lessens, and the cross section eventually becomes negligible for large deflection angles. Accordingly the intensity will be greatly reduced for the rays that suffer large deflection.

Care must be taken in using Fig. 6 to determine the angle distribution of the intensity of deflected rays. In practice, the incident rays are distributed in a finite spatial extent; and thus, the intensity of deflected rays will be nonzero within a finite angle. For an example, consider the incident rays that are uniformly distributed within  $y = b_1$  and  $b_2$  such that  $b_1 > b_2 > b_m$ . Let the deflection angles be denoted by  $\theta_1$  and  $\theta_2$ , respectively, for the rays with  $b_1$  and  $b_2$ . According to Fig. 3,  $\theta_2 > \theta_1$ , and all the rays are deflected into the angles between  $\theta_1$  and  $\theta_2$ . The intensity of the deflected rays is proportional to  $\sigma$  only within the angle lying between  $\theta_1$  and  $\theta_2$ . The intensity is zero outside these angles.

Plotted in Fig. 7 is the relation between the deflection angle  $\theta$  of a ray and the largest mean flow speed  $u_{\max}/c_{\infty}$  on the ray path. Many values of  $b$  and  $u_0$  were used in the calculations to produce these curves. All the calculations fall onto a single curve in each case of upstream propagation or downstream propagation. This feature can be recognized from the closed-form solution of the particle trajectory (see Eq. (A8)). Although the largest flow speed on a ray path is not known a priori, the almost perfect correlation will be useful for further studies of the flow gradient effects on an acoustic ray. For instance, one may be able to estimate the upper limit of the ray deflection for a given mean flow without a detailed calculation.

## CONCLUDING REMARKS

As noted in previous studies such as that in Ref. 13 (see Eq. (1) on p. 261 of ref. 13 or Eq. (10) in the present paper), the first order effect of the mean flow does not change an acoustic ray path in the absence of vorticity. The present investigation shows that, in a potential flow, deflection of an acoustic ray is a second-order effect of the mean flow and that the ray deflects in the direction of increasing mean flow speed regardless of the direction of the initial ray relative to the mean flow velocity.

The ray paths are, in many respects, similar to the trajectories of particles moving under the potential given in the form  $-(\gamma + 1)u^2/4$ . The various results for the particle motion are almost the same as those for the downstream rays and are characteristically similar to those for the upstream rays. Thus the closed form solution of the particle motion is very helpful in studies of the ray propagation in potential flow.

It is also shown that ray deflection is greater for upstream propagation than for downstream propagation. Flow in an inlet duct can often be assumed to be irrotational, and sound generated in the duct must propagate against the mean flow to be radiated. Consequently an initial conclusion might be reached that the directivity of sound radiation from such an inlet duct can be significantly affected by the mean flow gradients. However, it was also found that rays that experience large deflection suffer large reductions in intensity. Thus, in many practical problems, the ray deflection due to the potential flow gradients may not significantly alter the far-field radiation pattern. The consequences of this result will require further study using realistic inlet flow and sound sources.

The results mentioned herein are characteristically different from ray deflections in a sheared mean flow. In such a flow the first-order effect

involving vorticity is the dominant factor for deflection of acoustic rays. If a ray has a downstream component, the ray deflects in the direction of decreasing mean flow. An example is found in sound radiation from an exhaust flow duct. Such a duct involves a shear layer, in which the mean flow radially decreases.

## APPENDIX

### MOTION OF A CLASSICAL PARTICLE UNDER A CENTRAL FORCE FIELD

This Appendix deals with the motion of a classical particle of unit mass, which is governed by Eq. (13) with  $\vec{u}$  given in Eq. (12). Included herein are the equations for the particle trajectories and the functional relations between the parameters that are used in the text for the discussion of the numerical results.

With the substitution of Eq. (12), Eq. (13) is written as

$$\ddot{\vec{r}} = -\frac{\gamma + 1}{2} \frac{r_0^2 u_0^2}{r^3}. \quad (\text{A1})$$

The solution to this equation is well known.<sup>14</sup> Let the initial particle position be given by ( $x = -\infty$ ,  $y = b$ ) or by ( $r = \infty$ ,  $\theta = \pi$ ) and the initial velocity by  $\vec{v} = \hat{x}c_\infty$ . The trajectory of the particle is then determined as

$$r(\theta) = \frac{b(1 - \alpha)^{1/2}}{\sin[(1 - \alpha)^{1/2}(\pi - \theta)]}, \quad (\text{A2})$$

where

$$\alpha = \frac{\gamma + 1}{2} \left( \frac{u_0}{c_\infty} \right)^2 \left( \frac{b}{r_0} \right)^{-2}. \quad (\text{A3})$$

Here we have assumed that  $\alpha$  is less than unity. For  $\alpha \geq 1$ , the particle will be trapped into the center of the force. In other words the condition for an open trajectory is  $\alpha < 1$ , and one obtains, by using Eq. (A3),

$$\frac{b}{r_0} > \left( \frac{\gamma + 1}{2} \right)^{1/2} \frac{u_0}{c_\infty}. \quad (\text{A4})$$

An acoustic ray would also be trapped into the vortex center if the cylinder core were not present and  $b$  were smaller than a certain value (see Fig. 3 in Ref. 5).

Eq. (A2) possesses an infinite number of poles. However, only two poles are of physical significance. The pole at  $\theta = \pi$  corresponds to the initial position of the particle. Another pole corresponds to the final position, and the final polar angle is given by

$$\theta = \pi \left\{ 1 - \left[ 1 - \frac{\gamma + 1}{2} \left( \frac{u_0}{c_\infty} \right)^2 \left( \frac{b}{r_0} \right)^{-2} \right]^{-1/2} \right\}. \quad (A5)$$

The final angle is negative because the initial value of  $y$ ,  $b$ , is positive and the force is attractive. The absolute value of the final angle is equivalent to the deflection angle defined for acoustic rays.

At the turning point ( $r = r_c$ ,  $\theta = \theta_c$ ),  $dr/d\theta = 0$ . Thus

$$r_c = b(1 - \alpha)^{1/2}, \quad (A6)$$

$$\theta_c = \pi \left[ 1 - \frac{1}{2(1 - \alpha)^{1/2}} \right], \quad (A7)$$

with  $\alpha$  given in Eq. (A3).

The deflection angle can be expressed in terms of  $r_c$  as

$$|\phi| = \pi \left\{ \left[ 1 + \frac{\gamma + 1}{2} \left( \frac{u_{\max}}{c_\infty} \right)^2 \right]^{1/2} - 1 \right\}, \quad (A8)$$

where  $u_{\max} = u_0 r_0 / r_c$ .

Similarly to the case of the acoustic rays, one may define the minimum impact parameter  $b_m$  in such a way that  $r_c \geq r_0$  for  $b \geq b_m$  and  $r_c < r_0$  for  $b < b_m$ . One can obtain, by using Eq. (A6),

$$\frac{b_m}{r_0} = \left[ 1 + \frac{\gamma + 1}{2} \left( \frac{u_0}{c_\infty} \right)^2 \right]^{1/2}. \quad (A9)$$

The deflection cross section,  $\sigma = db/r_0 d\theta$ , is obtained by differentiating Eq. (A5) as

$$\sigma = \frac{2}{\pi(\gamma + 1)} \left( \frac{u_0}{c_\infty} \right)^{-2} \left[ \left( \frac{b}{r_0} \right)^2 - \frac{\gamma + 1}{2} \left( \frac{u_0}{c_\infty} \right)^2 \right]^{3/2}. \quad (\text{A10})$$

or

$$\sigma = \frac{1}{\pi} \left( \frac{\gamma + 1}{2} \right)^{1/2} \frac{u_0}{c_\infty} \left[ \left( 1 - \frac{\theta}{\pi} \right)^2 - 1 \right]^{-3/2}. \quad (\text{A11})$$

## REFERENCES

1. J. J. Colehour, "Transonic Flow Analysis Using a Streamline Coordinate Transformation Procedure," AIAA Paper No. 73-657 (July 1973).
2. L. D. Landau and E. M. Lifshitz, The Classical Theory of Fields (Addison-Wesley, Reading, MA, 1962), Rev. 2nd ed., ch. 7.
3. Y. C. Cho, "A Statistical Theory for Sound Radiation and Reflection from a Duct," *J. Acoust. Soc. Am.* 65, 1373-1379 (1979).
4. J. B. Keller, "Geometrical Theory of Diffraction," *J. Opt. Soc. Am.* 52, 116-130 (1962).
5. R. F. Salant, "Acoustic Rays in Two-Dimensional Rotating Flows," *J. Acoust. Soc. Am.* 46, 1153-1157 (1969).
6. T. M. Georges, "Acoustic Ray Paths Through a Model Vortex with a Viscous Core," *J. Acoust. Soc. Am.* 51, 206-209 (1972).
7. M. Born and E. Wolf, Principles of Optics (Pergamon Press, New York, 1969), 4th ed.
8. M. J. Lighthill, Waves in Fluids (Cambridge University Press, New York, 1978).
9. D. Blokhintzev, "The Propagation of Sound in an Inhomogeneous and Moving Medium I," *J. Acoust. Soc. Am.* 18, 322-328 (1946).
10. F. P. Bretherton and C. J. R. Garrett, "Wavestrains in Inhomogeneous Moving Media," *Proc. Roy. Soc., London, A.* 302, 529-554 (1968).
11. S. M. Candel, "Numerical Solution of Conservation Equations Arising in Linear Wave Theory: Application to Aeroacoustics," *J. Fluid Mech.* 83, 465-493 (1977).
12. W. D. Hayes, "Kinematic Wave Theory," *Proc. Roy Soc., London, A.* 302, 209-226 (1970).

13. L. D. Landau and E. M. Lifshitz, Fluid Mechanics (Addison-Wesley Pub. Co., Reading, MA, 1959), p. 259.
14. H. Goldstein, Classical Mechanics (Addison-Wesley Pub. Co., Reading, MA, 1950, ch. 3.

## FIGURE CAPTIONS

Figure 1. - Deflection pattern of acoustic rays in a free vortex with hard-wall cylinder core. In the left side, values of impact parameter  $b$  are given for incident rays that are all parallel to the  $x$ -axis. At the end of each ray path, the deflection angle of the ray measured from the  $x$ -axis is given. Mean flow speed,  $u_0/c_\infty$ , is 0.5.

Figure 2. - Correlation between mean flow speed and minimum impact parameter.

Figure 3. - Ray deflection angle as a function of mean flow speed for impact parameters  $b/r_0$  of 1.5, 3, and 6.

Figure 4. - Ray deflection angle as a function of impact parameter for mean flow speeds  $u_0/c_\infty$  of 0.5, 1, and 1.5.

Figure 5. - Deflection cross section as a function of impact parameter for mean flow speeds  $u_0/c_\infty$  of 0.5, 1, and 1.5.

Figure 6. - Deflection cross section as a function of deflection angle.

Figure 7. - Ray deflection angle as a function of maximum flow speed on ray path.

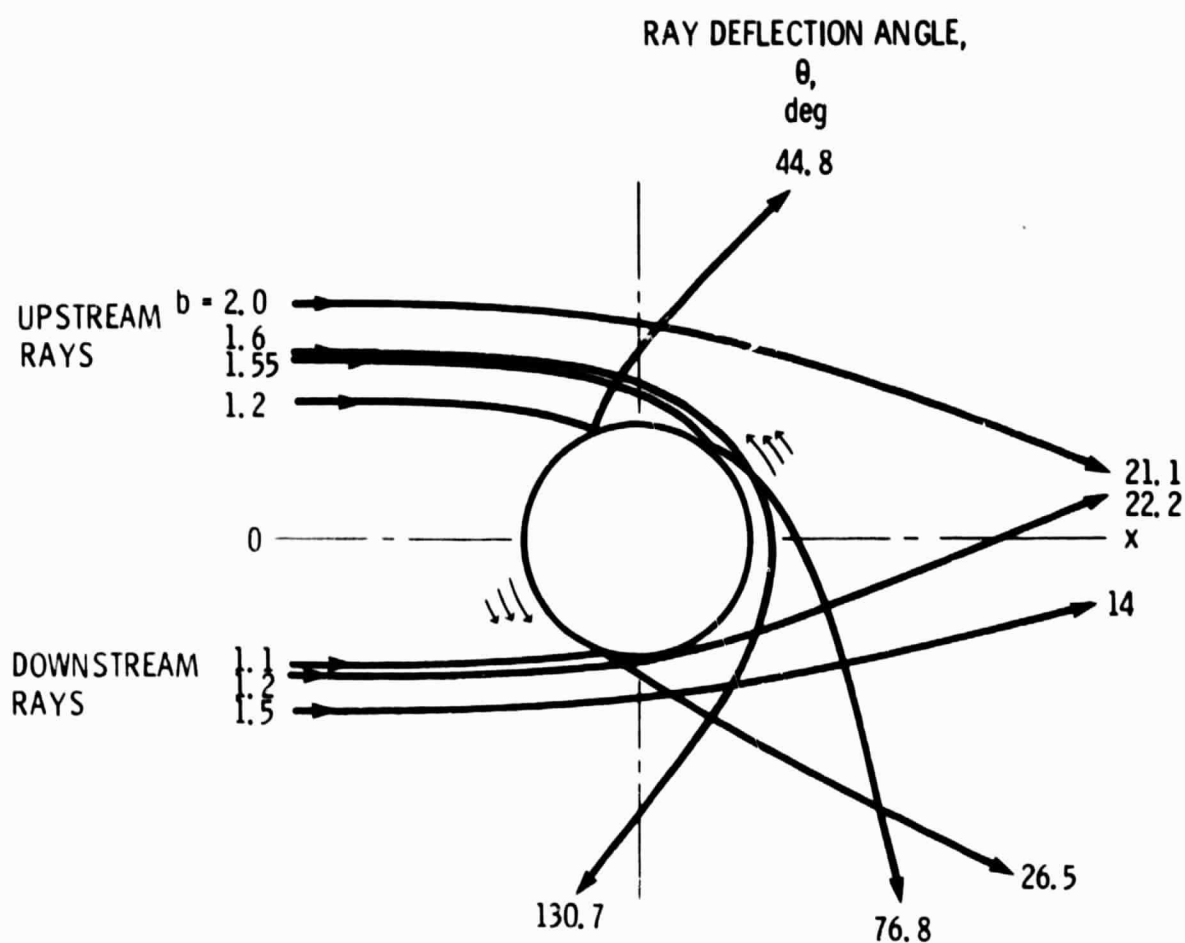


Figure 1. - Deflection pattern of acoustic rays in a free vortex with hard-wall cylinder core. In the left side, values of impact parameter  $b$  are given for incident rays that are all parallel to the  $x$ -axis. At the end of each ray path, the deflection angle of the ray measured from the  $x$ -axis is given. Mean flow speed,  $u_0/c_\infty$ , is 0.5.

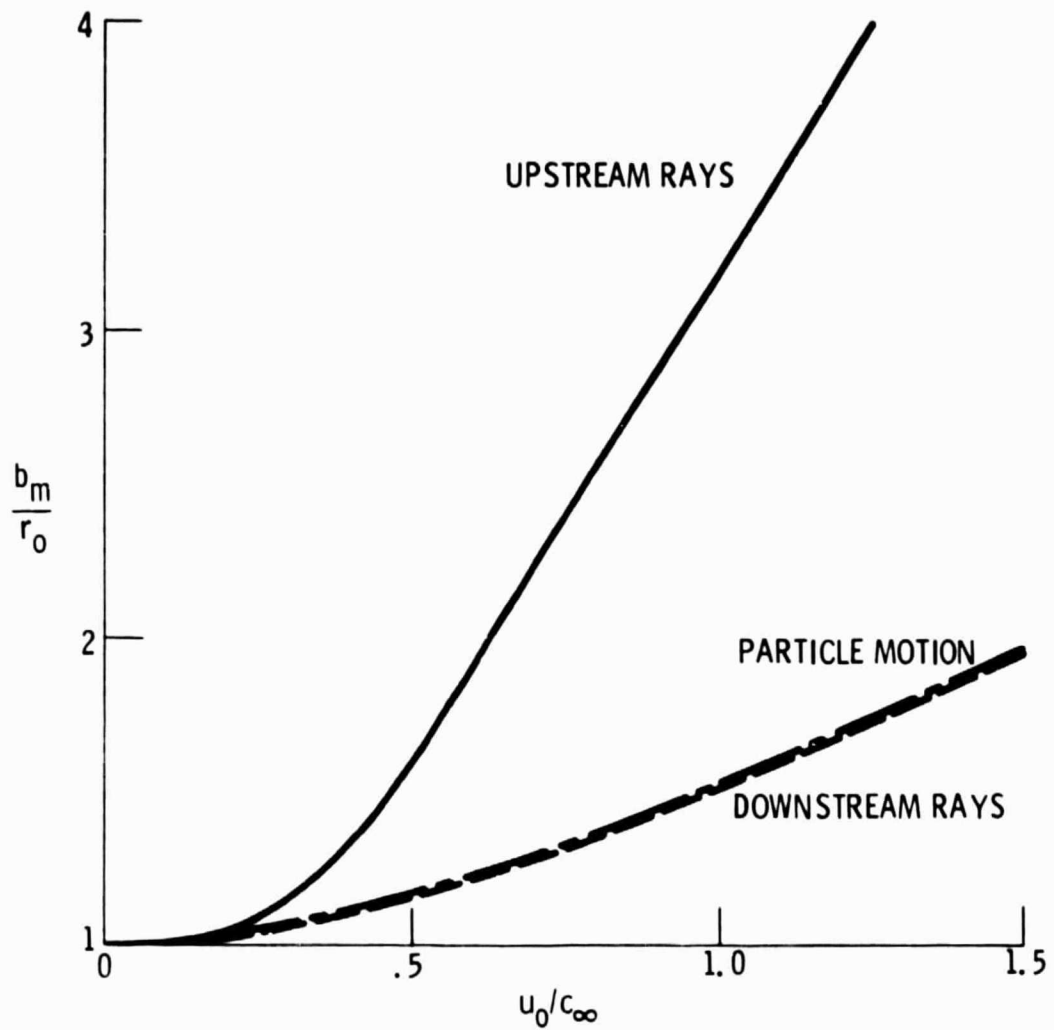


Figure 2. - Correlation between mean flow speed and minimum impact parameter.

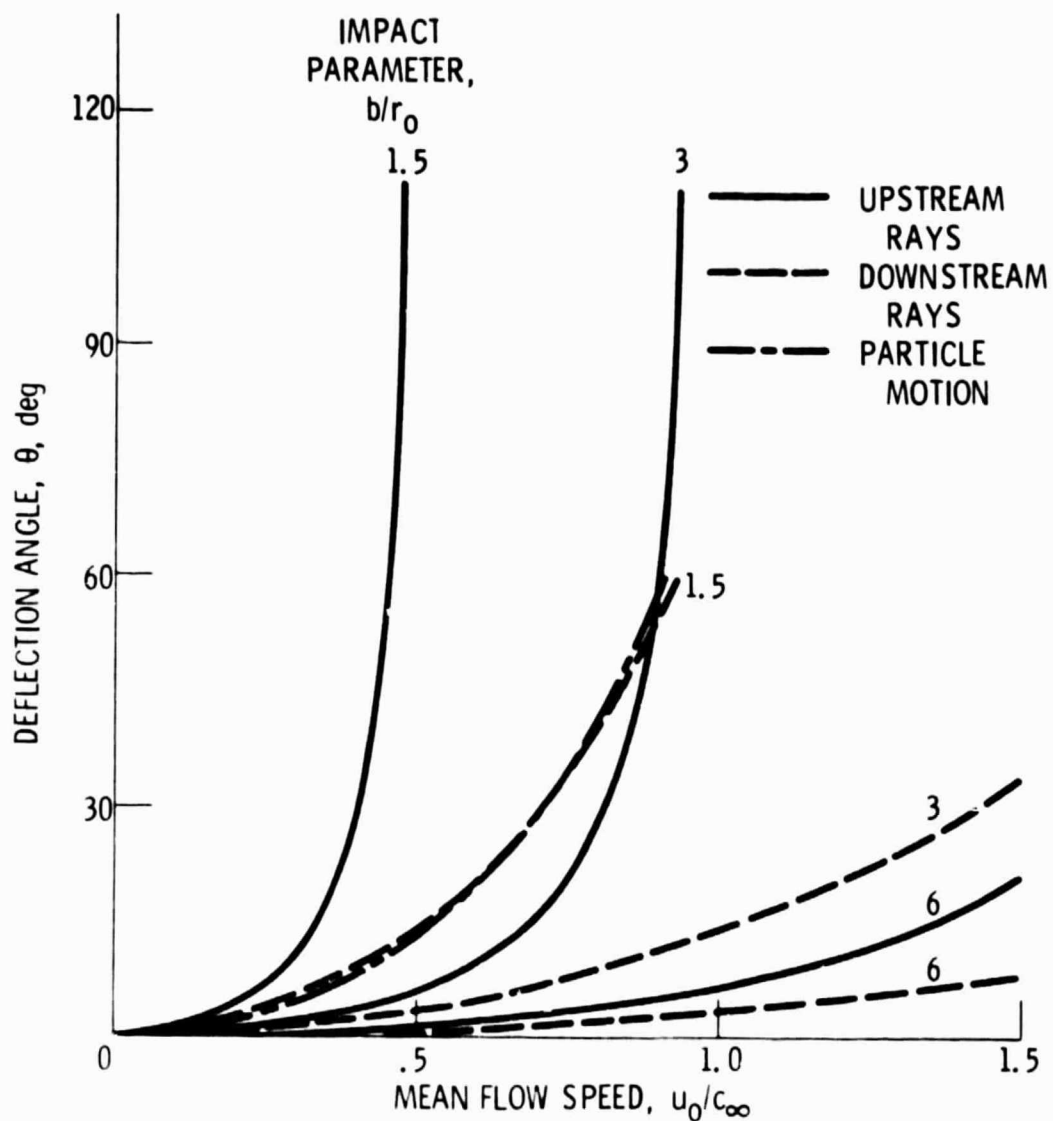


Figure 3. Ray deflection angle as a function of mean flow speed for impact parameters  $b/r_0$  of 1.5, 3, and 6.

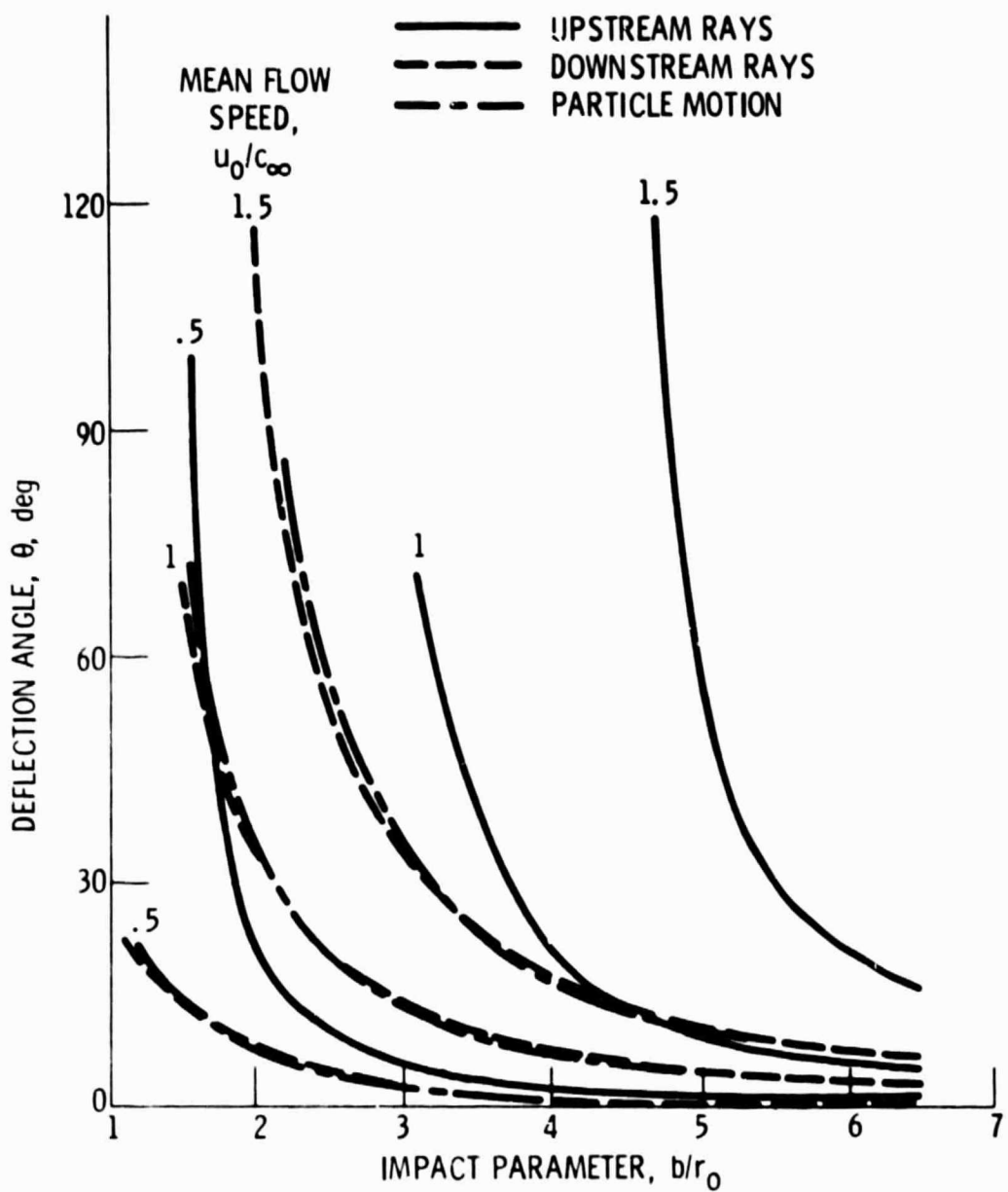


Figure 4. - Ray deflection angle as a function of impact parameter for mean flow speeds  $u_0/c_\infty$  of 0.5, 1, and 1.5.

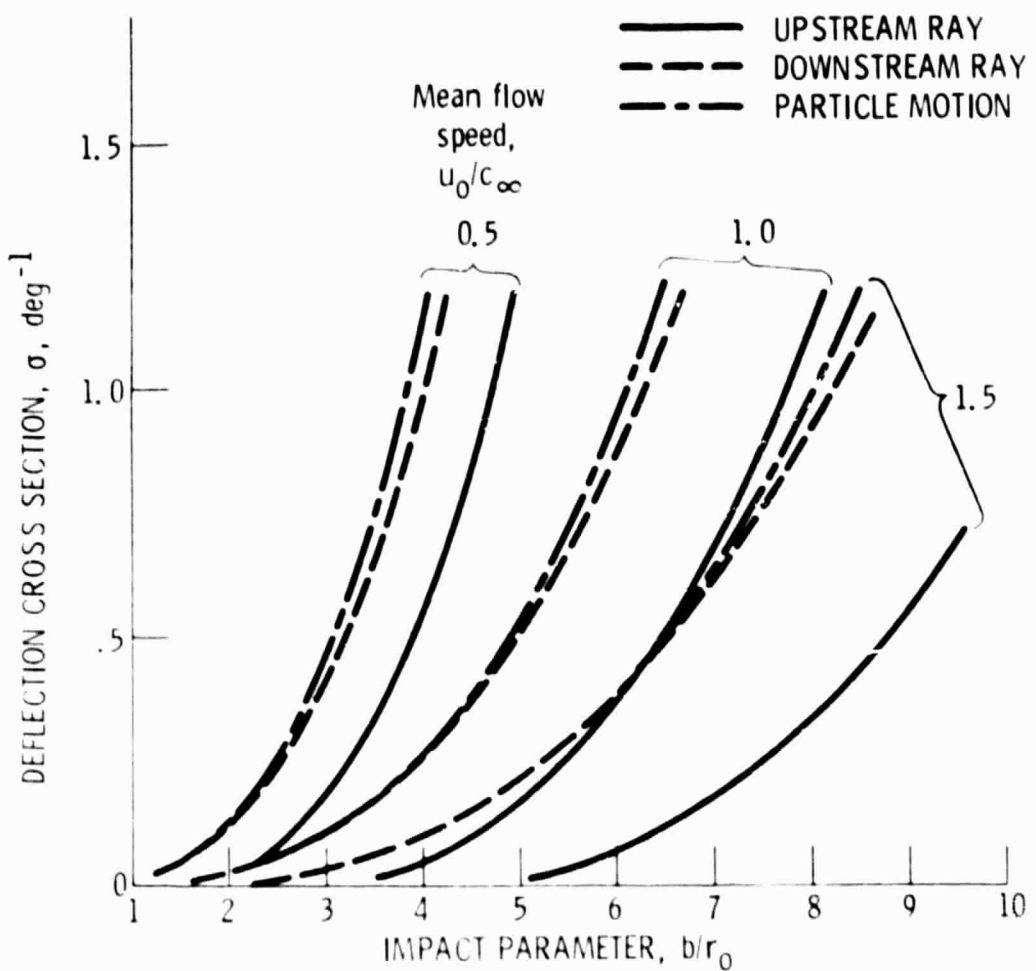


Figure 5. - Deflection cross section as a function of impact parameter for mean flow speeds  $u_0/c_\infty$  of 0.5, 1, and 1.5.

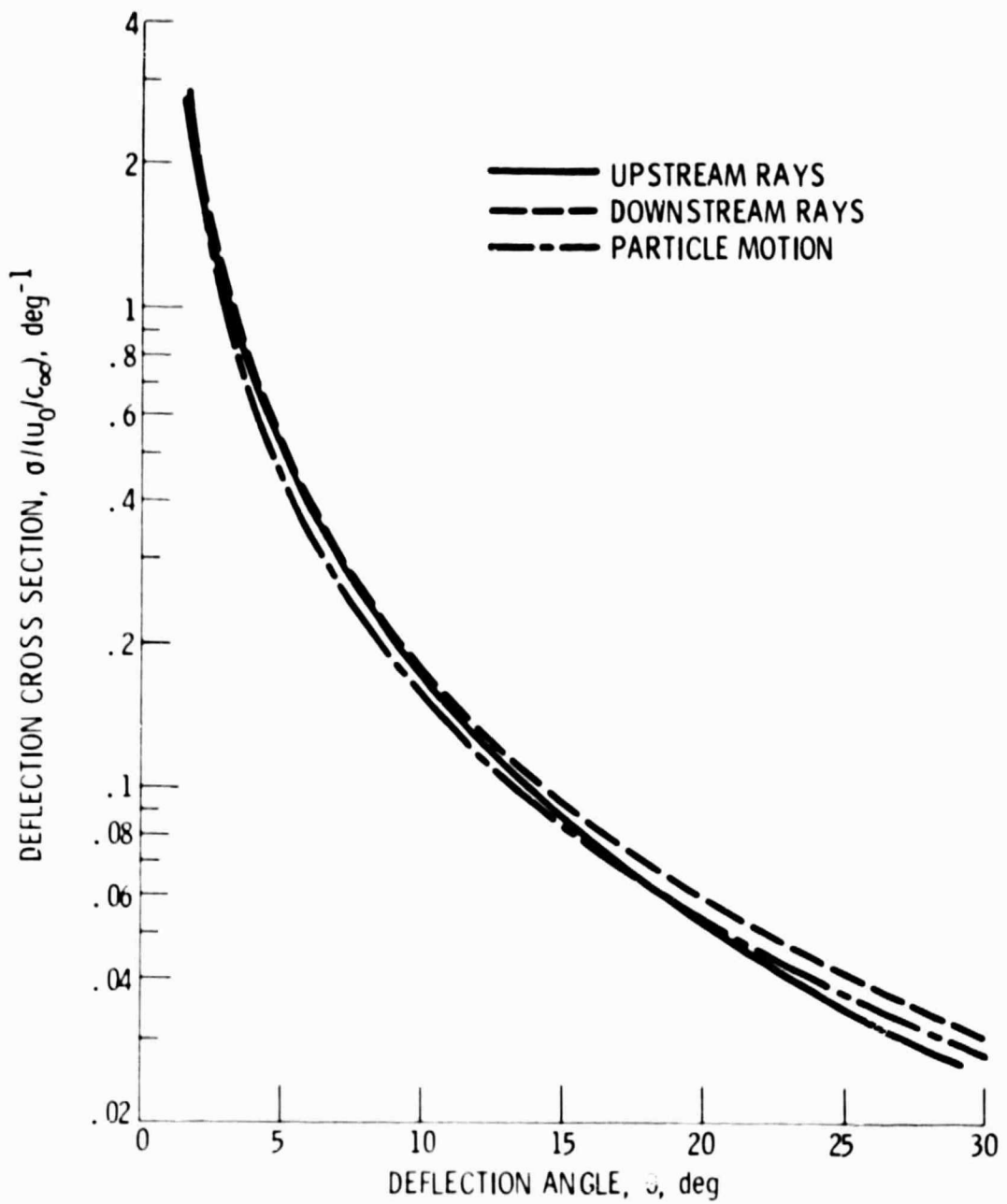


Figure 6. - Deflection cross section as a function of deflection angle.

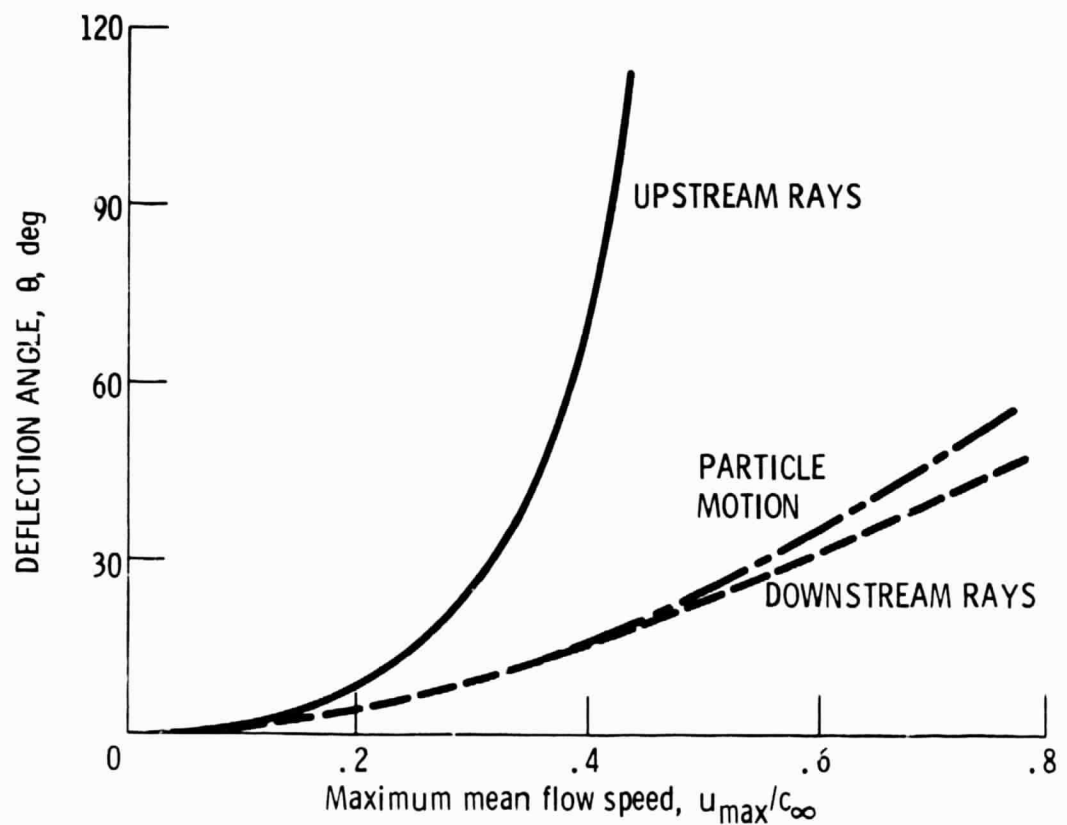


Figure 7. - Ray deflection angle as a function of maximum flow speed on ray path.